

Minimizing the Ground Effect for Photophoretically Levitating Disks

Zhipeng Lu,^{1,2,*} Miranda Stern,² Jinqiao Li,³ David Candia,² Lorenzo Yao-Bate,^{2,4} Thomas J. Celenza,² Mohsen Azadi,⁵ Matthew F. Campbell^{①,2} and Igor Bargatin^{①,2}


¹*Department of Chemistry, University of Pennsylvania, Philadelphia, PA 19104, USA*

²*Department of Mechanical Engineering and Applied Mechanics, University of Pennsylvania, Philadelphia, PA 19104, USA*

³*Department of Materials Science and Engineering, University of Pennsylvania, Philadelphia, PA 19104, USA*

⁴*Department of Physics, University of Pennsylvania, Philadelphia, PA 19104, USA*

⁵*Singh Center for Nanotechnology, University of Pennsylvania, Philadelphia, PA 19104, USA*

 (Received 13 September 2022; revised 20 February 2023; accepted 23 February 2023; published 3 April 2023)

Photophoretic levitation is a propulsion mechanism by which lightweight objects can be lifted and controlled through their interactions with light. Since photophoretic forces on macroscopic objects are usually maximized at low pressures, they may be tested in a vacuum chamber in close proximity to the chamber floor and walls. We report experimental evidence that the terrain under levitating microflyers, including the chamber floor or the launchpad from which the microflyer lifts off, can greatly increase the photophoretic lift forces relative to their free-space (midair) values. To characterize this so-called “ground effect” during vacuum-chamber tests, we introduce a miniature launchpad composed of three J-shaped (candy-cane-like) wires that minimize the microflyer’s extraneous interactions with the underlying surfaces. We compare our J-shaped-wire launchpad with previously used wire-mesh launchpads for simple levitating Mylar-based disks with diameters of 2, 4, and 8 cm. Importantly, we discover that wire-mesh launchpads increase the photophoretic lift force by up to sixfold. A significant ground effect is also associated with the bottom of the vacuum chamber, particularly when the distance to the bottom surface is less than the diameter of the levitating disk. We provide guidelines to minimize the ground effect in vacuum-chamber experiments, which are necessary to test photophoretic microflyers intended for high-altitude exploration and surveillance on Earth or on Mars.

DOI: [10.1103/PhysRevApplied.19.044004](https://doi.org/10.1103/PhysRevApplied.19.044004)

I. INTRODUCTION

Microflyers are typically defined as airborne vehicles with dimensions smaller than approximately 10 cm. Compared with conventional unmanned aerial vehicles (UAVs) such as weather balloons, drones, and satellites, microflyers are lightweight, low-cost, and use less energy. Some microflyers can be driven by wind or solar energy and may not need a battery, engine, or motor. Such miniaturized aerial vehicles can be dispersed by wind as plant-seed-inspired microrobots [1] or powered by the Sun using photovoltaics [2] or photophoretic levitation [3], potentially enabling applications in ubiquitous sensing and in monitoring of the atmosphere, climate, and local environment [4–6].

Although microflyers are typically intended for uses far from the ground, they may be tested in close proximity to horizontal surfaces, either solid or very sparse, such as a wire-mesh launchpad [3,7,8]. These underlying

surfaces can greatly modify the airflow in the vicinity of the microflyer, create an area of increased pressure under the microflyer, and enhance the lift force experienced by the microflyer in a phenomenon called the ground effect [9–11]. In the continuum regime, i.e., when the mean free path is much smaller than the flyer dimensions, the ground effect has been well studied for three-dimensional hovercraft and for aircraft that take off or cruise at very low altitudes. Previous researchers have focused mainly on how the enhanced lift can be used to address problems of flight security, fuel consumption [9,12], and control of miniorotorcraft [13].

The ground effect can also be significant in photophoretic levitation, as previously calculated for photophoresis of microscopic aerosol spheres close to a solid plane surface [14] and observed for macroscopic plates hovering on an air cushion at atmospheric pressure [7]. During testing of photophoretic microflyers, the mean free path is often comparable to the characteristic dimensions of the system, i.e., the experiments are done in the transition regime between free-molecular and continuum

*zplu@seas.upenn.edu

fluid dynamics. Note that the characteristic dimension of the system is unambiguous only in midair, where it is defined as the size of the levitating disk. If the disk is levitating close to another surface, we can define the characteristic size as the distance to that surface, the periodicity of that surface, etc. This implies that multiple Knudsen numbers, defined as the ratio of the mean free path to some characteristic dimension, can be relevant depending on the details of the experimental setup.

The ground effect results from a combination of free-molecular back-and-forth bouncing of air molecules between the flyer and the launchpad and continuum air flow (e.g., an elevated-pressure air cushion) [7,14]. The associated increase in the lift force can be particularly large when tests are done in a typical tabletop vacuum chamber, in which the distance to the nearest horizontal surface may be comparable to or even smaller than the characteristic size of the levitating vehicle. For macroscopic photophoretic flyers, the aerodynamic differences between laboratory test launchpads and the real-world midair environment may therefore lead to exaggerated expectations for the altitude range and payload capability of microflyers.

We present work characterizing the ground effect in the transition regime in this paper. Given the critical importance of accurate tests for the future deployment of photophoretic microflyers on the Earth or Mars, we quantify the impact of the ground effect for minimal J-shaped launchpads and the wire-mesh-based launchpads previously used, as described below.

II. EXPERIMENTAL RESULTS AND METHODOLOGY

We conduct the experiments in the present work using simple microflyers consisting of disk-shaped 0.5- μm -thick Mylar films with diameters of 2, 4, and 8 cm. These microflyers are chosen due to their ease of fabrication and adequate mechanical, thermal, and aerodynamic stability [3]. Our levitation mechanism relies on a difference in the thermal accommodation coefficient across these films, made possible by depositing a thin carbon-nanotube (CNT) film on the underside of the disk [3,15–21]. A representative 8-cm-diameter disk is shown in Fig. 1(d). We test our microflyers in an acrylic vacuum chamber positioned over an array of eight light emitting diodes (LEDs) as shown in Fig. 1(a), and also in Fig. 7. Our primary experimental variables are the light irradiance experienced by the microflyer and the vacuum-chamber pressure. As discussed in the Appendix, we carefully characterize the light irradiance in the vacuum chamber as a function of position, elevation, and any shading factors present (such as the launchpad) using a photodiode and an optical sensor.

When illuminated by incident light, the microflyer experiences (1) an upward photophoretic force, which may be enhanced by the ground effect, (2) a downward

gravitational pull, and (3) an electrostatic stiction force, which can be either repulsive (upward) or attractive (downward). The photophoretic force increases with the light irradiance and is typically maximized at pressures such that the mean free path is comparable to the disk diameter (i.e., for $0.01 < \text{Kn} < 10$, where Kn is the Knudsen number) [14]. As a result, for a given microflyer size, an optimal pressure exists at which the irradiance needed for liftoff is smallest. In a single experiment, we therefore increase the light irradiance until the microflyer lifts off, while holding the chamber pressure constant. This process is then repeated at different pressures to allow us to plot the liftoff irradiance versus pressure and determine the optimal pressure (Fig. 2). Making such irradiance-pressure plots for a variety of microflyers and launchpads allows us to infer the magnitude of the ground effect for each microflyer-launchpad combination. For instance, consider a case in which the minimum light irradiance required for liftoff at a given pressure increases when the launchpad is altered. Given the approximate linear relationship between the light irradiance and the photophoretic lift force in the transition regime [3,15], we can infer that the ground effect is reduced when the altered launchpad is used compared with the unmodified launchpad, as discussed below.

Observing liftoff in levitation experiments is facilitated by launchpads that elevate the microflyer and minimize electrostatic stiction forces associated with the chamber floor. Although it is not shown in the figures, we connect every launchpad to an electrical grounding circuit to minimize these electrostatic forces. Previously used launchpads [3,7] were composed of sparse steel-mesh grids that allowed a very high fraction of the incident light to pass through. The main geometric parameters of the mesh are the wire diameter d and wire spacing s , resulting in an open-area fraction $\Phi = s^2/(s+d)^2$ for a square mesh, as shown in Fig. 1(b). Note that as Φ approaches unity, the light shading caused by the mesh disappears, while the irradiance needed for liftoff should increase because the ground effect is minimized.

A. Minimizing launchpad-associated ground effect using minimal J-shaped-wire launchpad

To minimize the ground effect in the experiments described in this paper, we design a launchpad consisting of three inverted-J-shaped (i.e., candy-cane-like) wires that minimize the contact area with the microflyer, as shown in Fig. 1(c). We use wires drawn from previously used wire-mesh launchpads [as in Fig. 1(b)], but bend them into “J” shapes with a millimeter-scale radius of curvature at the top and maintain the same distance from the chamber floor to the disk as with the previously used mesh launchpads. A triad of wire canes inserted vertically into an aluminum ring holder provides the necessary

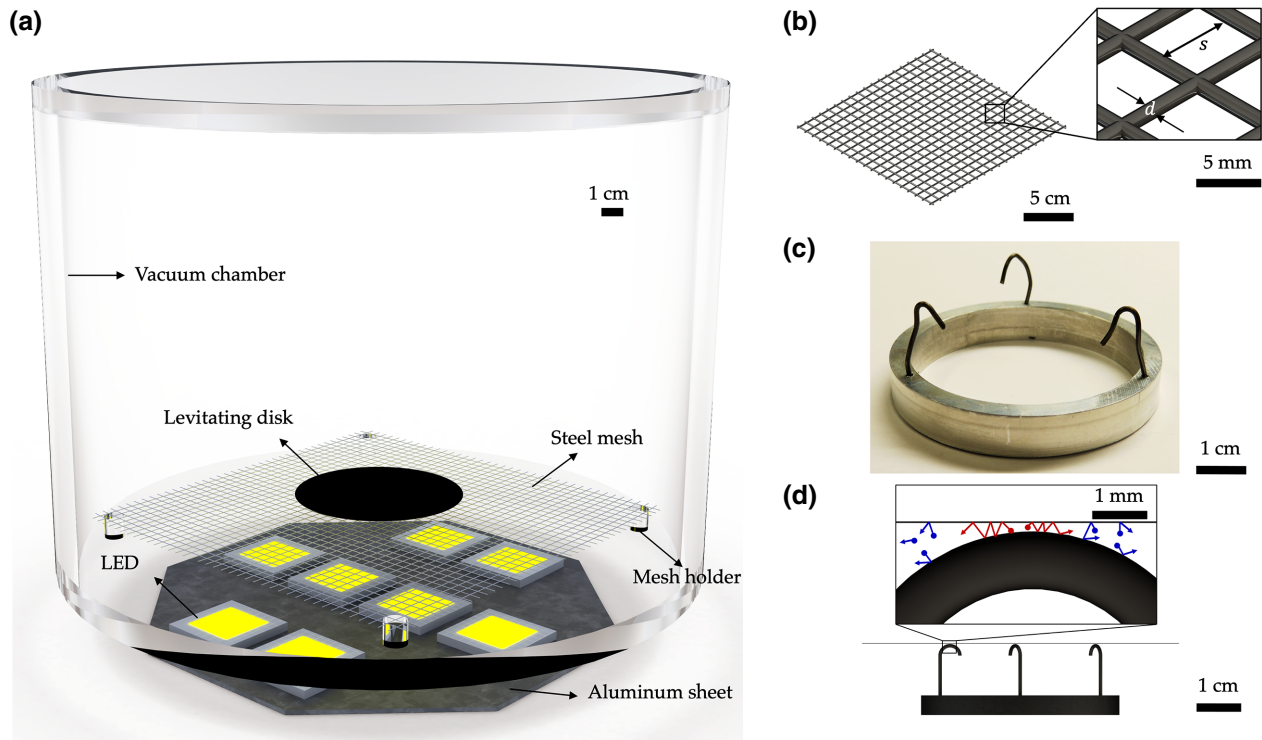


FIG. 1. Experimental setups for a wire-mesh and a J-shaped-wire launchpad and a microflyer. (a) Schematic diagram of experimental setup consisting of an acrylic vacuum chamber, an 8-cm-diameter CNT-Mylar-alumina microflyer, a piece of 73%-open steel mesh, and eight LEDs below the chamber. (b) Schematic diagram of a 0.9-mm-diameter 5.4-mm-spacing steel mesh, showing wire spacing s and diameter d . (c) Photograph of a triad of 0.9-mm-diameter J-shaped steel sticks and a holder ring. (d) Photograph of an 8-cm-diameter CNT-Mylar-alumina disk. The electrical grounding circuits for the two types of launchpad are not shown, for simplicity.

stability to support the microflyer before takeoff while minimizing the interfacial contact. The effective open area is greater than 99% even for the thickest (1.6-mm-diameter) wire and the smallest (2-cm-diameter) disk. Our experiments indicate that these ultrasparse launchpads exhibit a minimal ground effect due to the underlying J-shaped wires. In particular, we observe no dependence on the wire diameter for J-shaped-wire launchpads made from 0.23,

0.9, and 1.6-mm-diameter wires (Fig. 2), in contrast to the wire-mesh launchpads discussed later.

The absence of a ground effect can also be illustrated by looking at the *optimal Knudsen number*, defined as the Knudsen number corresponding to the pressure at which the irradiance needed for liftoff is minimized. The optimal Knudsen numbers in Fig. 2 are marked by dark-shaded intervals due to the uncertainty produced by

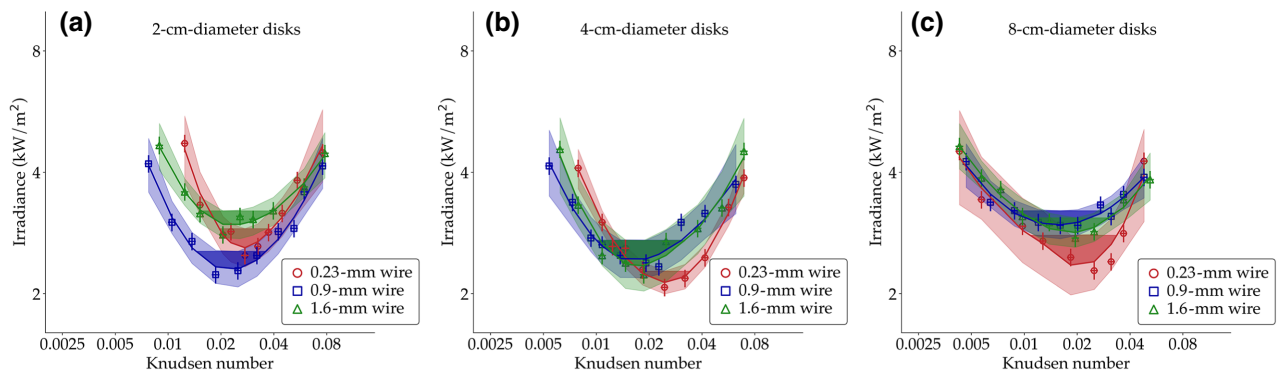


FIG. 2. Levitation performance of microflyers on J-shaped-wire launchpads with different wire diameters. The optimal Knudsen number can be seen to be independent of the microflyer diameter and the wire diameter. The microflyers are (a) 2-, (b) 4-, and (c) 8-cm-diameter alumina-Mylar-CNT disks. The solid lines show LOESS fits, with 99% confidence intervals shown by light shading. The optimal pressures are shown by darker shading.

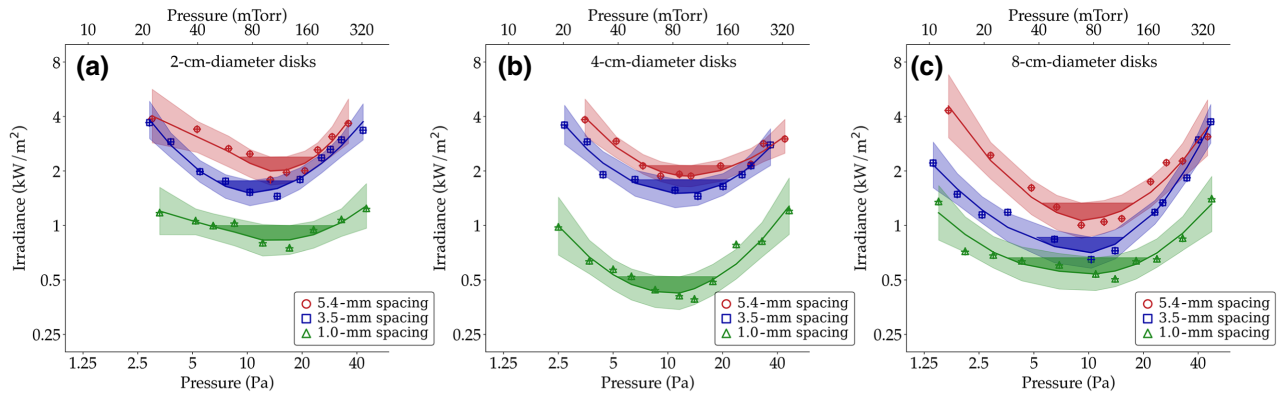


FIG. 3. Plots similar to those in Fig. 2, for steel meshes with a fixed wire diameter (0.9 mm) and different wire spacings but plotted versus the pressure. The optimal pressure can be seen to be independent of the wire spacing and the microflyer diameter. Note that the range of the irradiance axis is adjusted relative to Fig. 2 to show clearer patterns of the irradiance versus the Knudsen number.

experimental observation error and the locally estimated scatterplot smoothing (LOESS) algorithm that we use. As can be seen from the figure, all values overlap within experimental error. In particular, the optimal Knudsen number shows no dependence on either the diameter of the J-wire or the diameter of the microflyer itself, exactly as predicted by the theory of midair levitation [3]. Specifically, the average optimal Knudsen numbers for 2-, 4-, and 8-cm-diameter disks are centered around 0.025. Given the measurement uncertainty, the optimal Knudsen number is invariant, meaning that the mean free path at the optimal pressure is about 40 times smaller than the disk diameter in all cases. It is well known [14] that the midair photophoretic force is maximized in the transition regime for Knudsen numbers from 0.01 to 10, in agreement with our findings.

B. Large launchpad-associated ground effect for wire-mesh launchpads

In contrast to the J-shaped-wire launchpads described in Sec. II A, the wire-mesh launchpads that we used previously in Refs. [3,7] exhibit strong evidence of a

ground effect when we systematically vary the wire diameter and spacing of the mesh. First, we use three steel meshes with the same 0.9-mm wire diameter and wire spacings of 1.0, 3.5, and 5.4 mm, corresponding to open-area percentages of 28%, 63%, and 73%, respectively. For these experiments (Fig. 3), we plot the light irradiance versus the pressure rather than the Knudsen number because it is difficult to know in advance which characteristic dimension (diameter, mesh wire diameter, or spacing) should be used to define the Knudsen number. As can be seen from Fig. 3, the central values of the optimal pressure for all three spacings are approximately 12 Pa, with no obvious dependence on the wire spacing or the diameter of the microflyer disk.

As discussed in Sec. II A, without a ground effect, i.e., in midair, larger samples are predicted to have inversely proportionally lower optimal pressures than smaller samples, i.e., the optimal ratio of the mean free path to the diameter should be constant [14,15]. The fact that we observe this in Fig. 2 but not in Fig. 3 indicates the presence of a ground effect for wire-mesh launchpads. In addition, the minimum light irradiance increases as the steel mesh

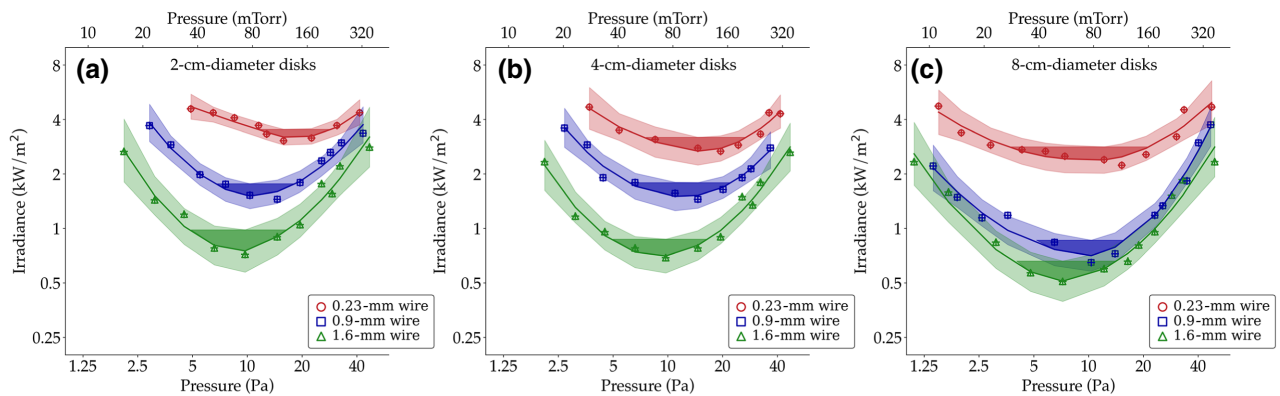


FIG. 4. As Fig. 3, but for steel meshes with a fixed wire spacing (3.5 mm) and different wire diameters. The optimal pressure decreases with increasing wire diameter (i.e., decreasing open area).

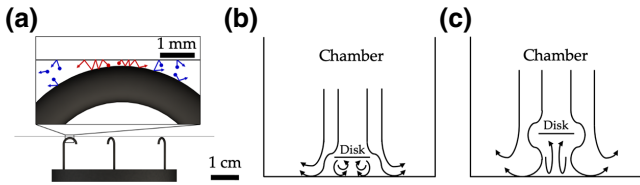


FIG. 5. Simplified features of gas dynamics between a microflyer and neighboring surfaces. (a) Cross-sectional schematic diagram of molecule trajectories during levitation on J-shaped steel sticks. (b),(c) Cross-sectional schematic diagrams of the air flow during levitation when the floor-to-disk distance is (b) smaller than the disk diameter and (c) greater than the disk diameter. In (a), red arrows represent molecules bouncing back and forth between the launchpad wire and the levitating disk, leading to the ground effect, while blue arrows represent other trajectories of air molecules.

becomes more open, because the launchpad-associated ground effect should vanish as the launchpad tends to 100% open area.

Next, we fix the wire spacing at 3.5 mm and vary the wire diameter instead (Fig. 4). The open-area percentages for the 0.23-, 0.9-, and 1.6-mm-diameter wires that we select are 88%, 63%, and 47%, respectively. As shown in Fig. 4, the optimal pressure decreases with both increasing wire diameter and increasing levitating-disk diameter, and, again, the minimum irradiance for liftoff increases as the mesh becomes more open, indicating a strong ground effect. However, the optimal pressure is not inversely proportional to either the mesh wire diameter or the levitating-disk diameter.

Instead, as the wire diameter is reduced by a factor of 7 (from 1.6 to 0.23 mm), the optimal pressure increases by approximately a factor of 2 for the smallest disk (2-cm diameter) and a factor of 1.5 for the intermediate-size disk, and does not significantly change for the largest disk. Similarly, as the disk diameter is reduced by a factor of 4

(from 8 to 2 cm), the optimal pressure changes by a factor of approximately 2 for the thinnest-wire mesh (0.23 mm), but does not change measurably for the two less open meshes (0.9- and 1.6-mm wire diameter). Therefore, no single Knudsen number can serve as a nondimensional invariant, and both of these characteristic dimensions are important.

Clearly, the ground effect is strongest for the largest disks and the largest mesh wire diameters. For the thickest (1.6-mm-diameter) wires, the minimum required irradiances can be seen to be up to 6 times lower for meshes than for the J-shaped wire launchpads. Since the light irradiance scales approximately linearly with the photophoretic lift force in the transition regime [3,15], for a specific microflyer with a given weight, this sixfold decrease in irradiance is approximately equivalent to a six-fold enhancement of the photophoretic lift force due to the ground effect.

In contrast, for the thinnest-wire mesh (0.23-mm diameter) and the smallest disk size (2-cm diameter), the optimal pressure and minimum intensity for the wire-mesh launchpads in Fig. 4 are very similar to those observed with the minimal J-shaped-wire launchpads described in Sec. II A (Fig. 2). These results are corroborated by the fact that we did not detect any large differences between 73%-open and 85%-open meshes (both high open-area percentages) in our previous experiments [3], which were also done with very small samples (with diameters of 0.6 cm). The decreasing influence of the ground effect with increasing open area suggests that ideal launchpads should be very sparse, especially for the largest samples.

The basic mechanism by which a wire mesh increases the photophoretic lift force on a microflyer, i.e., the ground effect, can be described as follows. In the slip-flow or transitional flow regime, air molecules behave as a combination of free molecules and a continuum fluid depending on the specific conditions. As shown in Fig. 5(a), for closely located horizontal surfaces where the mean free

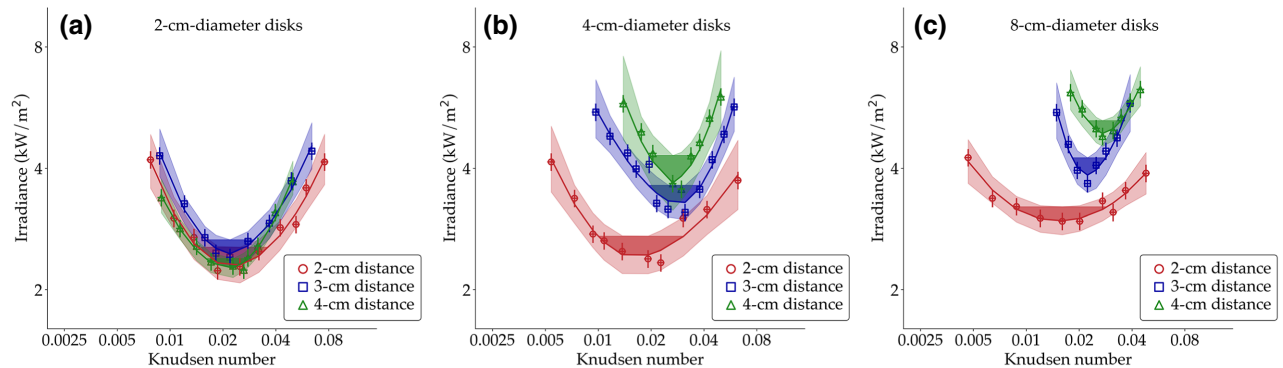


FIG. 6. As Fig. 2, but for cane-shaped steel sticks with a fixed wire diameter (i.e., 0.9 mm) and different distances to the chamber floor. The optimal Knudsen number can be seen to be dependent on the floor-to-disk distance when that distance is smaller than the disk diameter.

path is larger than the intersurface spacing, air molecules can bounce back and forth more frequently between the two surfaces, imparting recoil forces that are larger than those experienced by a microflyer in midair. Immediately before takeoff, the disk rests on the launchpad and the wire diameter determines the typical distance that the molecules travel when bouncing back and forth between the levitating disk and the launchpad; this sets a characteristic length scale and explains why the optimal pressure depends on the wire diameter. The magnitude of the ground effect also gradually decreases with increasing open area of the mesh and eventually vanishes as the open area approaches 100%. Therefore, as the underlying surface becomes increasingly sparse, the dependence on the open-area percentage and the wire diameter becomes insignificant, the optimal pressure instead begins to depend on the size of the levitating disk, and the optimal Knudsen number stays at around 0.025. We note that rigorous modeling of the observed ground effect requires computer-intensive numerical modeling in the transition regime [12,22,23], which is beyond the scope of this experimentally focused manuscript.

C. Floor-associated ground effect

Even with ultrasparse J-shaped-wire launchpads, which by themselves produce no measurable ground effect, other underlying surfaces may produce a floor-associated ground effect due to their vertical proximity to the microflyer [24,25]. After the launchpad, the second closest horizontal surface for any sample is typically the floor of the vacuum chamber. To investigate the associated ground effect, we prepare J-shaped sticks with lengths of 2, 3, and 4 cm and change the vertical distance between the sample and the bottom surface of the vacuum chamber while maintaining the vertical distance between the LEDs and the sample (by moving the chamber itself) to keep the light irradiance on the microflyer constant. Similarly to the case for large aerial vehicles such as rotorcraft and hovercraft [9–13], this type of ground effect results from the underlying surface deflecting the airflow around the microflyer downward and thus creating an area of higher pressure (i.e., an air cushion) under the microflyer, as sketched in Figs. 5(b) and 5(c).

As shown in Fig. 6, the smallest (2-cm-diameter) disk has very similar optimal Knudsen numbers and irradiances regardless of the floor-to-microflyer distance, while the 4- and 8-cm-diameter microflyers both have higher optimal Knudsen numbers and minimum light irradiances as the distance grows. In this case, we can denote the two Knudsen numbers determined by the microflyer diameter and the floor-to-disk distance by Kn_{diam} and Kn_{dist} , respectively. Our experiments indicate that the floor-associated ground effect due to the chamber bottom gradually decreases as the distance from the disk to the chamber bottom increases, and becomes insignificant when that

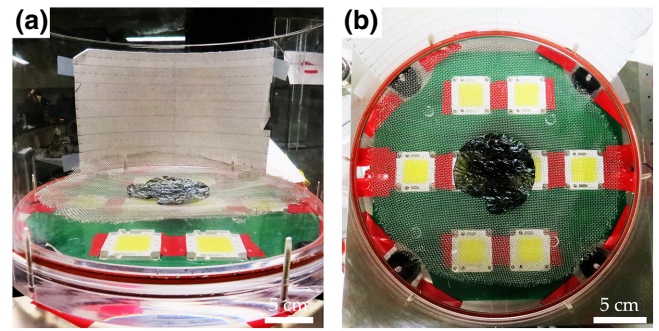


FIG. 7. Photographs of experimental setup consisting of an acrylic vacuum chamber, an 8-cm-diameter CNT-Mylar-alumina microflyer, a piece of 73%-open steel mesh, and eight LEDs below the chamber. (a) Side view. (b) Top view.

distance exceeds the disk diameter (i.e., $Kn_{\text{diam}} > Kn_{\text{dist}}$). In other words, the larger of the two Knudsen numbers controls the optimal pressure more, and, in midair, only the diameter-based Knudsen number matters.

III. CONCLUSIONS

Based on these experimental results, we suggest the following guidelines when testing microflyers in vacuum chambers. First, the launchpad-associated ground effect should be minimized by making the launchpad so sparse that the optimal pressure no longer depends on the parameters of the launchpad and instead scales with the size of the microflyer. Second, the distance between the vacuum-chamber floor and the microflyer must be increased until the pressure-irradiance curves cease to show a dependence on the vertical distance. Typically, this distance needs to be larger than the largest dimension of the levitating structure to minimize the floor-associated ground effect. We note, finally, that the ground effect in the transition regime, which is typical in photophoretic experiments, exhibits aerodynamic features of both the free-molecular and the continuum regimes (Fig. 5).

In summary, we demonstrate that photophoretic microflyers tested in relatively small vacuum chambers can experience large ground effects associated with both the supporting launchpad structure and the chamber bottom, which may lead to greatly exaggerated expectations of the photophoretic lift force in midair applications. We develop a minimal launchpad consisting of J-shaped steel sticks that is nearly 100% open so as to make the impact of the launchpad-associated ground effect insignificant, as indicated by the fact that the irradiance–Knudsen-number graphs are independent of the wire diameter. We then characterize steel-mesh launchpads with different wire diameters and spacings, where we observe stronger ground effects for denser meshes. Furthermore, we vary the distance between the microflyer disks and the bottom surface of the vacuum chamber, concluding that the distance

between the microflyer and any other underlying surface should be at least as large as the diameter of the disk to minimize the floor-associated ground effect. We highlight the complexity of choosing the characteristic dimension and Knudsen number of the system as a function of the microflyer diameter, the launchpad dimensions, and the floor-to-microflyer distance. Minimizing the ground effect in laboratory tests of photophoretic microflyers is important for developing realistic expectations for the payloads of photophoretic UAVs in the Earth's mesosphere or the atmosphere of Mars.

DATA AVAILABILITY STATEMENT

The data that support the findings of this study are available from the corresponding author upon reasonable request.

ACKNOWLEDGMENTS

This work is partly supported by the NSF under Grant No. CBET-1845933, the NASA Space Technology Graduate Research Opportunity under Grant No. 80NSSC20K1191, and the School of Engineering and Applied Science at the University of Pennsylvania. This work was carried out in part at the Singh Center for Nanotechnology, which is supported by the NSF National Nanotechnology Coordinated Infrastructure Program under Grant No. NNCI-2025608.

AUTHOR CONTRIBUTIONS

Zhipeng Lu: conceptualization (equal); methodology (equal); resources (lead); investigation (lead); data curation (lead); formal analysis (equal); software (lead); writing—original draft (lead). *Miranda Stern*: resources (lead); investigation (supporting). *Jinqiao Li*: resources (supporting); software (supporting). *David Candia*: resources (supporting). *Lorenzo Yao-Bate*: investigation (supporting). *Thomas J. Celenza*: resources (supporting); investigation (supporting). *Mohsen Azadi*: conceptualization (supporting); methodology (supporting); software (supporting). *Matthew F. Campbell*: writing—review and editing (supporting). *Igor Bargatin*: conceptualization (equal); formal analysis (equal); writing—review and editing (lead).

The authors have no conflicts to disclose.

APPENDIX: MATERIALS AND METHODS

1. Procedure for microflyer fabrication

We start with a 0.5- μm -thick Mylar sheet (DuPont), whose area density is approximately 0.7 g/m^2 as measured on an analytical balance (A&D HR-202). We wrap the film around a 525- μm -thick silicon wafer and spin-coat a solution of 0.2% (weight) water-based single-wall CNTs (1–2 nm in diameter and 5–30 μm in length, NanoAmor) on

the top surface at 300 revolutions per minute for 10 s. We bake the resulting bilayer structure on a hotplate at 90 °C for 10 min. By weighing the samples, we determine the areal density to be 0.9–1.3 g/m^2 after this step. We then flip the Mylar-CNT film and deposit a layer of 100-nm-thick alumina via atomic layer deposition (Cambridge Nanotech S2000 ALD) at 140 °C using water and $\text{Al}_2(\text{CH}_3)_6$ as precursors. Last, we use laser micromachining (IPG IX280-DXF) to cut circular disks with diameters of 2, 4, and 8 cm. The areal density of the final alumina-Mylar-CNT disks is typically 1.2–1.6 g/m^2 .

2. Procedure for vacuum-chamber testing

We use a customized 10-l cylindrical vacuum chamber with an acrylic body and steel flanges, as pictured in Figs. 7. A two-stage (roughing-turbo) vacuum pump (Pfeiffer HiCube 80 Eco Turbo Pumping Station) allows us to reach chamber pressures between 0.8 and 200 Pa, as measured by a vacuum-gauge sensor (InstruTech, Inc., CVG101GF). In the experiments using metal meshes, the meshes are electrically grounded to minimize electrostatic forces. In the experiments using J-shaped steel sticks, we add a 1-mm-thick polyethylene terephthalate film coated with indium tin oxide (Adafruit) underneath the ring holder to provide electrical grounding. This optically transparent and electrically conductive film forms an effective and convenient electrical grounding circuit with approximately 85% optical transparency (we account for this partial absorption when calculating the actual irradiance on the microflyers). We set up an eight-LED (LOHAS LH-XP-100W-6000K) array to create a symmetric, uniform, and sufficiently intense light source that can be tuned continuously with a power supply (Teyleten Robot Non-Isolated Step-Up Module). Finally, we apply a thin layer of silver paste (Arctic Silver 5 Polysynthetic Thermal Compound) between the LEDs and the aluminum base plate to enhance the heat dissipation from the LED array.

3. Procedure for characterization of light irradiance

The whole LED array can safely provide light irradiances of up to 7 kW/m^2 (absent any shadowing from the launchpad), as measured using optical power and energy sensors. The methodology can be described as follows: (1) using collimated light from the LED array to establish an equivalence of the signals from a fully open photodiode (Vishay Semiconductors Silicon PIN Photodiodes Osram BPW34) and a partially open optical sensor (Thorlabs, Inc., S305C and PM100USB); (2) finding the percentage of light received by the optical sensor by repeating step 1 but using the original light from the LED array; and (3) measuring the light irradiance with the percentage obtained in step 2 considered. Note that the shadowing effect of every launchpad is characterized, and both the photodiode and the optical sensor are precalibrated.

4. Experimental results of previous publications

Cortes *et al.* [7] reported photophoretic levitation of nanocardboard rectangular plates on a micropatterned 0%-open glass substrate and an 84%-open wire mesh. The plates were 6×13 mm in dimensions and 0.1 mg in weight. The levitation height was 10 mm. We argue that the launchpad and floor-associated ground effects arising from the glass launchpad were potentially large, while those arising from the 84%-open wire-mesh launchpad were much less significant.

Azadi *et al.* [3] reported photophoretic levitation of circular disks on a 74%-open wire mesh and an 85%-open wire mesh. The disks were 6 mm in diameter and 0.03 mg in weight. The levitation height was about 5 mm. We argue that the launchpad and floor-associated ground effects arising from the two meshes were not large and, reasonably, led to only slight differences in the experimental results.

-
- [1] B. Kim, K. Li, J. Kim, Y. Park, H. Jang, X. Wang, Z. Xie, S. Won, H. Yoon, G. Lee, and W. Jang, Three-dimensional electronic microfliers inspired by wind-dispersed seeds, *Nature* **597**, 503 (2021).
- [2] N. Jafferis, E. Helbling, M. Karpelson, and R. Wood, Untethered flight of an insect-sized flapping-wing microscale aerial vehicle, *Nature* **570**, 491 (2019).
- [3] M. Azadi, G. Popov, Z. Lu, A. Eskenazi, A. Bang, M. Campbell, H. Hu, and I. Bargatin, Controlled levitation of nanostructured thin films for sun-powered near-space flight, *Sci. Adv.* **7**, eabe1127 (2021).
- [4] I. Colomina and P. Molina, Unmanned aerial systems for photogrammetry and remote sensing, *J. Photogrammetry Remote Sens.* **92**, 79 (2014).
- [5] S. Nam and G. Joshi, Unmanned aerial vehicle localization using distributed sensors, *Int. J. Distrib. Sens. Netw.* **13**, 1550147717732920 (2017).
- [6] Y. Cao, W. Yu, W. Ren, and G. Chen, An overview of recent progress in the study of distributed multi-agent coordination, *IEEE Trans. Ind. Inform.* **9**, 427 (2012).
- [7] J. Cortes, C. Stanczak, M. Azadi, M. Narula, S. Nicaise, H. Hu, and I. Bargatin, Photophoretic levitation of macroscopic nanocardboard plates, *Adv. Mater.* **32**, 1906878 (2020).
- [8] C. Powers, D. Mellinger, A. Kushleyev, B. Kothmann, and V. Kumar, *Influence of Aerodynamics and Proximity Effects in Quadrotor Flight* (Springer, Heidelberg, 2013), p. 289.
- [9] K. Rozhdestvensky, Wing-in-ground effect vehicles, *Prog. Aerosp. Sci.* **42**, 211 (2006).
- [10] C. Han, J. Cho, Y. Moon, Y. Yoon, and Y. Song, Design of an arolevitation electric vehicle for high-speed ground transportation system, *J. Aircr.* **42**, 93 (2005).
- [11] Y. Moon, H. Oh, and J. Seo, Aerodynamic investigation of three-dimensional wings in ground effect for aero-levitation electric vehicle, *Aerosp. Sci. Technol.* **9**, 485 (2005).
- [12] A. Matus-Vargas, G. Rodriguez-Gomez, and J. Martinez-Carranza, Ground effect on rotorcraft unmanned aerial vehicles: A review, *Intell. Serv. Robot.* **14**, 99 (2021).
- [13] P. Wei, S. Chan, S. Lee, and Z. Kong, Mitigating ground effect on mini quadcopters with model reference adaptive control, *Int. J. Intell. Robot. Appl.* **3**, 283 (2019).
- [14] H. Keh and F. Hsu, Photophoresis of an aerosol sphere normal to a plane wall, *J. Colloid Interface Sci.* **289**, 94 (2005).
- [15] H. Rohatschek, Semi-empirical model of photophoretic forces for the entire range of pressures, *J. Aerosol Sci.* **26**, 717 (1995).
- [16] N. Tong, Photophoretic force in the free molecule and transition regimes, *J. Colloid Interface Sci.* **43**, 78 (1973).
- [17] C. Loesche and T. Husmann, Photophoresis on particles hotter/colder than the ambient gas for the entire range of pressures, *J. Aerosol Sci.* **102**, 55 (2016).
- [18] D. Gilbey, A re-examination of thermal accommodation coefficient theory, *J. Phys. Chem. Solids* **23**, 1453 (1962).
- [19] P. Feuer, Theory of the thermal accommodation coefficients of a diatomic gas, *J. Chem. Phys.* **39**, 1311 (1963).
- [20] W. Trott, D. Rader, J. Castaneda, J. Torczynski, and M. Gallis, Measurement of gas-surface accommodation, *AIP Conf. Proc.* 1084, 621 (2008).
- [21] M. Grau, F. Völklein, A. Meier, C. Kunz, J. Heidler, and P. Woias, Method for measuring thermal accommodation coefficients of gases on thin film surfaces using a MEMS sensor structure, *J. Vac. Sci. Technol. A: Vac., Surf., Films* **34**, 041601 (2016).
- [22] E. Kadivar and E. Kadivar, Computational study of the laminar to turbulent transition over the SD7003 airfoil in ground effect, *Thermophys. Aeromechanics* **25**, 497 (2018).
- [23] T. Barber and S. Hall, Aerodynamic ground effect: A case study of the integration of CFD and experiments, *Int. J. Vehicle Design* **40**, 299 (2006).
- [24] Q. Qu, P. Zuo, W. Wang, P. Liu, and R. Agarwal, Numerical investigation of the aerodynamics of an airfoil in mutational ground effect, *AIAA J.* **53**, 3144 (2015).
- [25] T. Anh, N. Binh, and J. Song, In-ground-effect model based adaptive altitude control of rotorcraft unmanned aerial vehicles, *IEEE Robot. Autom. Lett.* **7**, 794 (2021).